KICS The Korean Institute of Communications and Information Sciences

Available online at www.sciencedirect.com
ScienceDirect
ICT Express 5 (2019) 31–36
www.elsevier.com/locate/icte

Adaptive threshold and optimal frame duration for multi-taper spectrum sensing in cognitive radio

Ahmed O. Abdul Salam[a,*], Ray E. Sheriff[a], Saleh R. Al-Araji[b,1], Kahtan Mezher[b], Qassim Nasir[c]

[a] *Faculty of Engineering and Informatics, University of Bradford, Bradford, BD7 1DP, UK*
[b] *College of Engineering, Khalifa University of Science and Technology, P.O. Box 127788, Abu Dhabi, United Arab Emirates*
[c] *College of Engineering, University of Sharjah, P.O. Box 27272, Sharjah, United Arab Emirates*

Received 12 October 2017; received in revised form 29 January 2018; accepted 12 February 2018
Available online 19 March 2018

Abstract

This paper delivers an accurate approximation for adaptive threshold and optimal frame detection algorithms based on the robust multi-taper method aiming at an efficient spectrum sensing in cognitive radio systems. An appropriate adaptive thresholding allows for seamless vacation of unlicensed secondary users from certain bands upon primary users' requests, while arbitrary optimal frame detection contributes to the computational and throughput demands. Simulation exercises corroborate the given analysis over Rayleigh channel and multiple-input multiple-output configuration and emphasize the critical role of adopting applicable adaptive threshold and optimal frame detection policies.

Keywords: Cognitive radio; Spectrum sensing; Multi-taper; Adaptive threshold; Optimal sensing duration

1. Introduction

The trend of modern life at present has witnessed unprecedented online services and applications offered through wireless communication systems. A challenging situation has thus been created due to the scarcity of sufficient frequency spectrum that is capable of accommodating all of the intended demands. The Federal Communication Commission (FCC) agency has publicized the IEEE 802.22 standard in response to this problem [1]. To avail this standard, opportunistic unlicensed secondary users (SUs) can cohabit the same sub-bands of licensed primary users (PUs) given the restriction of causing no harm or disturbance. The use of cognitive radio (CR) has gained considerable attention as a highly competent approach that can support spectrum solutions. CR systems are responsive to their environment, process the knowledge and adequately adjust their internal parameters [2]. SUs equipped with CR systems continuously monitor the presence of PUs with a limited number of noisy readings. The existence of underutilized sub-bands is adherent to the PUs' dynamic activities of random pattern behavior. The SUs are to perform spectrum sensing (SS) either successively or sporadically so that they can instantly stop their broadcast upon PUs reappearance.

Proliferated surveys aspiring the SS in wireless CR systems are widely accessible in the literature; only two notable reviews are quoted here [3,4]. The SS algorithm comprises spectrum estimation (SE) and decision making. The term SE will be given preference here since major SS algorithms commonly share the same decision policy, while mostly differ in the quantification of spectrum entries. Without loss of generality, the SE techniques can be segregated into three main divisions. The first division is called as "guided SS", where both signal and noise information is provided, and under which the likelihood ratio test (LRT), the matched filter (MF), and the cyclostationary detection (CSD) techniques can be branded. The second division is called "semi-guided" or "semi-blind"

* Corresponding author.
E-mail address: aoa_salam@yahoo.com (A.O. Abdul Salam).
[1] Formerly at College of Engineering, Khalifa University of Science and Technology, United Arab Emirates.
Peer review under responsibility of The Korean Institute of Communications and Information Sciences (KICS).

https://doi.org/10.1016/j.icte.2018.02.002

SE, where only the noise information is known, and the energy detection (ED) and wavelet-based sensing can be put under this division. While the third division is called "unguided" or "blind" SS, where no prior information is provided and the emerging maximum to minimum eigenvalue (MME), covariance (COV), and blindly combined ED detections are identified. Each of these SE methods has certain drawbacks [3,4] and therefore none of them progressed any further herein.

An alternative SE scheme based on the non-parametric multi-taper method (MTM) was the focus of several studies [2,5,6]. The MTM has a particular ingredient called Slepian tapers that are orthonormal and have maximal energy concentrated in their main lobes. Thereby, they employ orthogonal data sets to achieve balanced tradeoffs in the bias–variance dilemma to enhance the SE resolution. The SE based on MTM, which will simply be called as MTSE, has an outstanding performance unlike any other in the same family. This is chiefly due to the robust spectrum leakage control governed by the tapering process.

On the other hand, the issue of adaptive threshold (AT) and optimal frame detection (OFD) is a challenging task in the decision making of SS in CR systems [7,8]. The SS performance at any point in time is highly determined by the values of performance metric probabilities, which in turn are reliant on the threshold and frame duration settings. A suitably selected detection threshold and frame length can minimize SS error, furnish PUs with proper protection, and improve spectrum utilization efficiency. Aiming at the targeted probability and threshold metrics, a subtle OFD necessary for SS in CRNs needs to be closely examined, as emphasized in earlier studies [9,10]. Such AT and OFD alterations may constitute a strategic role in the cooperative transmitter and receiver association [11].

1.1. Contributions

The novel contributions of this paper can be mainly summarized as given below

- Systematically approach the multiple-input multiple-output (MIMO) channel modeling and employ singular value decomposition (SVD) in the design of the proposed MTSE algorithm.
- Apply the quadrature form approximation to derive the MTSE based on MIMO that aims at improving the SE performance under low SNR regime.
- Adopt the framework of Neyman–Pearson (NP) hypothesis test to develop the close-form expressions for the MTSE–MIMO statistical measures.
- Derive the optimum AT and OFD algorithms necessary for efficient PUs protection and spectrum reuse policies by applying arbitrary utilization factors.
- Assess the variations between the above AT and OFD algorithms based on MTSE with respect to other methods employing traditional ED schemes [7–11].

1.2. Paper organization

This paper is organized as follows. Section 2 covers MIMO signal modeling and Section 3 presents MTSE structure. Section 4 presents the hypothesis test, while Section 5 discusses AT and OFD policies. Simulation results are provided in Section 6 followed by concluding remarks.

1.3. Mathematical annotations

The following annotations are used throughout this work: boldface uppercase letters for matrices; non-boldface uppercase letters for scalars; boldface lowercase letters for vectors, and; non-boldface lowercase letters denote scalar variables. The operators $(.)^{\mathrm{T}}$, $(.)^{*}$, $(.)^{\mathrm{H}}$, and $\|.\|_{\mathrm{F}}$ are for transpose, complex conjugate, Hermitian and Frobenius norm, respectively, while $\mathcal{j} = \sqrt{-1}$ stands for the imaginary prefix.

2. MIMO signal model

MIMO is employed to enhance the signal power and throughput and, eventually, the quality of service (QoS). The space–time block code (STBC) slightly deviates from MIMO by having the coding matrix formed instead of channel matrix. The analysis given here applies equally for both configurations with minor exceptions under particular conditions. Assume a wireless channel is of block flat-fading Rayleigh effect, the sensing time is considered shorter than the channel coherence time so that the channel gain $h_{i,j}$ is time-invariant upon sensing. A complex constellation of K sequence length is applied to this channel using N_t transmit and N_r receive antennas. The normalized baseband signal at the ith receive antenna is denoted by [5]

$$y_i(k) = \sum_{j=1}^{N_t} h_{i,j} x_j(k) + w_i(k), \nabla i \in [1, N_r], k \in [1, K] \quad (1)$$

and the $N_r \times N_t$ quasi-static channel matrix is given by

$$\mathbf{H} = \begin{bmatrix} h_{1,1} & h_{1,2} & \dots & h_{1,N_t} \\ h_{2,1} & h_{2,2} & \dots & h_{2,N_t} \\ \vdots & \vdots & \ddots & \vdots \\ h_{N_r,1} & h_{i,j} & \dots & h_{N_r,N_t} \end{bmatrix}. \quad (2)$$

Ignoring the time index briefly for simplicity, the model in (1) can take the following linear matrix form

$$\mathbf{Y} = \mathbf{HX} + \mathbf{W} \quad (3)$$

where $\mathbf{Y}$ is the received components from all N_r antennas, $\mathbf{X}$ is the $N_t \times 1$ complexed valued constellation with single symbol variance σ_x^2 and the additive noise $\mathbf{W}$ of size $N_t \times 1$ is an independent and identically distributed (i.i.d.) zero-mean circularly symmetrical complex Gaussian (ZMCSCG) denoted by $\mathcal{CN} \sim (0, \sigma_w^2 \mathbf{I}_{N_r})$, where $\mathbf{I}$ is the square identity matrix of order N_r. All these random variables are considered uncorrelated and independent of each other.

The MIMO signal model can be retrieved using a space–time matched filter (STMF) of the form $\mathbf{H}^*$. The SVD can also be used to simplify the channel into single-input single-output (SISO) components [2,5]. Applying the maximum ratio combining (MRC) for signal enhancement over a Hermitian channel reveals

$$y(k) = \mathbf{H}^*\mathbf{Y} = \|\mathbf{H}\|_F^2 x(k) + w(k). \quad (4)$$

Therefore, the linear MIMO model is reduced to a set of $R = \min(N_t, N_r)$ equivalent and independent parallel channels with coefficients $\|\mathbf{H}\|_F^2$, while the noise remains intact. The $\lambda = \|\mathbf{H}\|_F^2 = \text{diag}[\lambda_1, \lambda_2, \ldots, \lambda_R]$ are channel eigenvalues where $\lambda_r \geq 0$ is sorted in descending order ($\lambda_r \geq \lambda_{r+1}$). The model in (4) is revised for all virtual parsed channels, yielding

$$y(k) = \sum_{r=1}^{R} \lambda_r x(k) + w(k). \tag{5}$$

3. MTSE structure

The MTSE employs robust Slepian tapers of varying length to control the bias–variance tradeoffs and maximize the spectral concentration within a desirable bandwidth B. The first few $L \approx 2KB$ of these tapers are more powerful than the rest. Also, L represents the degree of freedom (DoF) to control the SE variance and the range of integers between 3-to-6 for its value is realistically sufficient for the design.

Normalizing some weighting factors, the Fast Fourier Transform (FFT) of the received data sequence for particular Slepian tapers $\{\upsilon_l\}_{k=0}^{K-1}$ and the corresponding eigen spectrum (power spectral density (PSD)) estimate are denoted by [2,5,6]

$$Y_l(f) = \frac{1}{K} \sum_{k=0}^{K-1} y(k)\upsilon_l(k) e^{-\jmath 2\pi f k} \tag{6}$$

$$\hat{S}_y(f) = \frac{1}{LK} \sum_{l=1}^{L-1} \sum_{k=0}^{K-1} \psi_l \left| y(k)\upsilon_l(k) e^{-\jmath 2\pi f k} \right|^2 \tag{7}$$

where ψ_l is the weighting eigenvectors of eigenspectrum. The following variable vectors can be defined [5,6]

$$\begin{aligned} \boldsymbol{\upsilon}_l &= [\upsilon_l(1), \upsilon_l(2), \ldots, \upsilon_l(K)]^{\mathrm{T}} \\ \boldsymbol{y} &= [y(1), y(2), \ldots, y(K)]^{\mathrm{T}} \\ \mathbf{a} &= \left[e^{\jmath 2\pi f}, e^{\jmath 2\pi f 2}, \ldots, e^{\jmath 2\pi f K}\right]^{\mathrm{T}} \end{aligned} \tag{8}$$

where $\mathbf{b}_l = \boldsymbol{\upsilon}_l \odot \mathbf{a}$ and $\odot$ refers to the Hadamard product. Substituting (8) in (6) reveals $Y_l(f) = \mathbf{b}_l^H y$, which when used together with the Slepian tapers will alter (7) to have the PSD estimate reinstated using quadrature form representation

$$\hat{S}_y(f) = \sum_{r=1}^{R} \lambda_r \boldsymbol{y}^H \boldsymbol{\Omega} \boldsymbol{y} \tag{9}$$

where $\boldsymbol{\Omega}$ is $L \times L$ idempotent matrix defined as $\boldsymbol{\Omega} = \sum_{l=0}^{L-1} \psi_l \mathbf{b}_l \mathbf{b}_l^H$. The above scalar PSD estimate can be viewed as the sum of individual PSD estimates computed over dominant tapers.

4. Hypothesis test

The binary hypothesis test (BHT) is adopted to decide between two observations, $\mathcal{H}_0$ and $\mathcal{H}_1$. The $\mathcal{H}_0$ is valid in case of a PU is actually absent, otherwise the $\mathcal{H}_1$ is valid when a PU is actually present. The statistics associated with these observations are the probabilities of false alarm P_{FA} and correct detection P_D, respectively. Given a sufficient test cost function signified by $\hat{S}_y(f)$, the framework of Neyman–Pearson (NP) optimal criterion defines the following decision rule

$$\begin{aligned} P_{FA} &= \Pr\left\{ \hat{S}_y(f) > \eta \,|\mathcal{H}_0 \right\} \\ P_D &= \Pr\left\{ \hat{S}_y(f) > \eta \,|\mathcal{H}_1 \right\} \end{aligned} \tag{10}$$

where η is a threshold calculated against the required constant false alarm rate (CFAR). The CFAR method is commonly used in practice when the test statistic and optimal threshold are unaffected by scaling the received sequence and noise of unknown power. The central limit theory (CLT) is valid for large data extents, hence the BHT takes the following form, noting that all constants either cancel each other or are normalized

$$\begin{aligned} &\text{Decide: } \mathcal{H}_0 \text{ if } \hat{S}_y(f) \approx^d \sigma_w^2 \chi_{RLK}^2 \\ &\text{Decide: } \mathcal{H}_1 \text{ if } \hat{S}_y(f) \approx^d \left(\sigma_s^2 + \sigma_w^2\right) \chi_{RLK}^2 \end{aligned} \tag{11}$$

where $\approx^d$ stands for "equal in distribution" by definition and χ_{RLK}^2 is the Chi-square distribution with RLK degrees of freedom. That is normal variables naturally converge into Chi-square statistics while passing through Rayleigh channels. The asymptotes of [7,8] can be directly worked out to consider the new characteristics of MTSE–MIMO combination and produce

$$\begin{aligned} P_{FA} &= Q\left\{ \frac{\eta - RLK\sigma_w^2}{2\sigma_w^2\sqrt{RLK/2}} \right\} \\ P_D &= Q\left\{ \frac{\eta - RLK(\sigma_x^2 + \sigma_w^2)}{2(\sigma_x^2 + \sigma_w^2)\sqrt{RLK/2}} \right\} \end{aligned} \tag{12}$$

where $Q(.)$ is the right tail cumulative distribution function and is given by $Q(z) = \frac{1}{2\pi} \int_z^\infty e^{-\frac{t^2}{2}} dt$. Let the SNR equal to $\gamma = \sigma_x^2/\sigma_w^2$ and with simple rearrangement of these two probabilities yields

$$\begin{aligned} P_{FA} &= Q\left\{ \frac{\acute{\eta} - RLK}{2\sqrt{RLK/2}} \right\} \\ P_D &= Q\left\{ \frac{\acute{\eta} - RLK(\gamma + 1)}{2(\gamma + 1)\sqrt{RLK/2}} \right\} \end{aligned} \tag{13}$$

where the revised threshold $\acute{\eta} = \eta/\sigma_w^2$ and the noise is of wide sense stationary (WSS) type. The results depicted in (12) and (13) signify the new probability measures attributed to the MTSE–MIMO interaction. These results slightly differ from those merely relying on the ED schemes under the same signaling environment [7–11].

5. Adaptive threshold & optimum duration

Generally, conventional SS designs are either based on the CFAR or constant detection rate (CDR) performance metrics. The CFAR sustains better spectrum reuse, while the CDR retains better protection for PUs against prohibited interferences from SUs. Both methods, however, produce constant performance indicators regardless of the SNR or noise power variations. In order to make it more rewarding for both PUs and SUs, an adequate AT policy needs to be devised to achieve the best trade-off between P_D and P_{FA} under various operational conditions.

Recent studies have suggested the weighted tradeoff principle (WTP) for minimizing the decision error probability of

SS [7,8], which is adopted in this work. The optimum threshold value has to be chosen to minimize the following convex function of total error decision probability, or occasionally called "utility function"

$$P_E = \alpha P_{FA} + (1-\alpha) P_{MD} \tag{14}$$

where the miss-detection probability is $P_{MD} = 1 - P_D$. A predefined preference weighting factor (spectrum utilization) $0 < \alpha < 1$ attains trade-off between the two probabilities (P_{MD}, P_{FA}). Substituting (13) in (14) yields

$$\begin{aligned} P_E = {} & \alpha Q\left\{\frac{\acute{\eta} - RLK}{2\sqrt{RLK/2}}\right\} + (1-\alpha) \\ & \times \left(1 - Q\left\{\frac{\acute{\eta} - RLK\,(\gamma+1)}{2\,(\gamma+1)\sqrt{RLK/2}}\right\}\right). \end{aligned} \tag{15}$$

Applying the first partial derivative with respect to $\acute{\eta}$ and equating it to zero achieves the minimization of (15), subject to the second derivative being greater than zero. The new MTSE–MIMO and utilization factor definitions aspire the following quadrature expression

$$\begin{aligned} & \left((\gamma+1)^2 - 1\right)\acute{\eta}^2 - 2RLK\gamma(\gamma+1)\acute{\eta} \\ & \quad - 4RLK(\gamma+1)^2 ln\left\{\frac{\alpha}{(1-\alpha)}\right\} = 0 \end{aligned} \tag{16}$$

and solving for the positive threshold to obtain the below

$$\acute{\eta} = RLK\frac{1 + \sqrt{1 + \frac{4}{RLK}\left(\frac{\gamma+2}{\gamma}\right) ln\left(\frac{\alpha}{(1-\alpha)}\right)}}{(\gamma+2)/(\gamma+1)}. \tag{17}$$

For large sequence length approaching infinity $RLK \to \infty$, the asymptote below can easily be conceived, which is a revised replica compared to that given in [7]

$$\acute{\eta} \approx 2RLK(\gamma+1)/(\gamma+2). \tag{18}$$

A fair value of $RLK \approx 100$ and higher is considered sufficient for the above asymptote to be valid. As can be seen from the last two expressions that the threshold value is largely administered by the SNR alternations and hence an adequate adaptation policy needs to be further explored. The above derivations are based on setting one threshold value only. This is commonly known as a one-stage AT, which differs than that of multiple-stage threshold schemes.

The proposed AT policy can be attained by knowing in advance the values of spectrum utilization factor α, SNR and the sequence length K. Hence, for arbitrary values of such parameters, the varying effect of different spectrum utilization α on the performance of the error decision probability can be analyzed by substituting (17) into (14) and the adaptation can be inferred accordingly.

On the other hand, it is also of primary objective to optimize the minimum sensing duration to facilitate maximum achievable throughputs of CR network (CRN) without blocking PUs. This is a crucial task to allow SUs to smoothly vacate their sub-bands upon PUs detection in overlay CRNs. Subsequent to the derivations approach of collision duration ratio (CDR) proposed in [9,10], this task can be computed for any priori given pair of (P_{MD}, P_{FA}) and complex signaling in the perspective of MTSE–MIMO. The minimum number of sensing samples can be obtained by canceling out the threshold parameter from both probability expressions [9,10]. Therefore, after canceling the threshold parameter from (13) and solving for the minimum number of sequence points needed for the detection frame, this obtains

$$K_{min} = \frac{2}{RL\gamma^2}\left[Q^{-1}(P_{FA}) - (\gamma+1)\,Q^{-1}(P_D)\right]^2. \tag{19}$$

It is therefore apparent that the minimum sensing interval, or OFD, is inversely related to the parameters of MTSE–MIMO structure. That means increasing the number of antennas, tapers and second exponent of the SNR value will reduce the number of sequence samples required to achieve successful detection and higher throughputs. The inverse proportionality with respect to SNR exponent is of great impact and would be highly desirable if it can be straightly done, but due to various constraints this option is not always feasible in reality.

6. Simulation results

The above theoretical analysis is numerically evaluated after using the following common simulation settings. It is assumed a binary-shift keying (BPSK) sequence of $K = 1024$ samples applied to MTSE with $L = 3$ Slepian tapers and equipped with 2×2 MIMO configuration and through flat-fading Rayleigh channel. The total number of effective points within the processing frame is equal to 6144 in this case, which surely rises as the complexity of MTSE–MIMO increases while maintaining the signal sequence intact. Therefore, the asymptotic approximation of (18) is evidently met.

The performance of detection threshold is firstly assessed with reference to SNR variations from −25 dB to 0 dB, and arbitrary utilization factors $\alpha = 0.1$, 0.5 and 0.9. The value $\alpha = 0.5$ symbolizes the separation line unraveling two preferences maintaining; better spectrum reuse (larger α) or additional PU protection (smaller α). Three threshold trends are thus generated as per expression (17), while the fourth trend represents the asymptotic threshold behavior described in (18) and all plotted in Fig. 1.

Fig. 1 infers several observations that are worth looking at. (1) The asymptotic threshold trend is in exact alignment with the threshold trend of $\alpha = 0.5$. (2) All threshold trends are concentrated and sharply climbing with respect to the incremental SNR beyond 0 dB and irrespective of α. This means the received SNR value is relatively large enough to readily bring the requirement of appropriate spectrum reuse and PUs protection correspondingly applicable. (3) The threshold trends for $\alpha >< 0.5$ exhibit a symmetrical distribution centered at the asymptotic and $\alpha = 0.5$ threshold trends. (4) The threshold trends for $\alpha > 0.5$ are also mounting for SNR less than 0 dB. This seems logical to set for larger threshold values in order to secure better PUs protection designated by larger values of α. Keep in mind that the utilization factor of (14) and (17) in this paper is allocated different to what was given in (Eqs. (6) and (11) of [7]). However, the compilation of (14) and (17) is consistent with that given in (Eqs. (9) and (12)

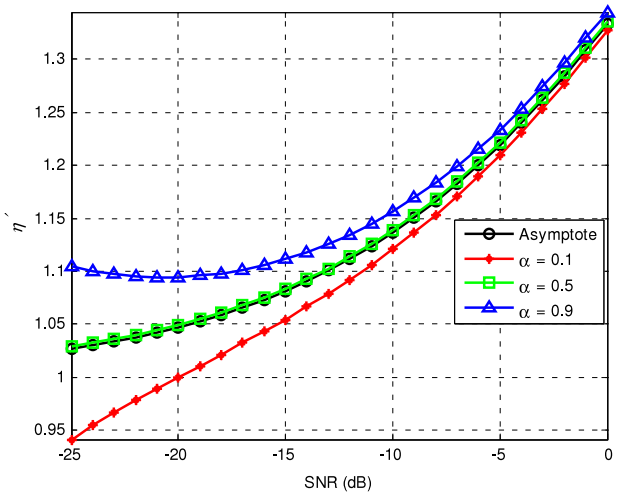

Fig. 1. Detection threshold against variations in SNR γ: Asymptote and selected values of utilization factor α.

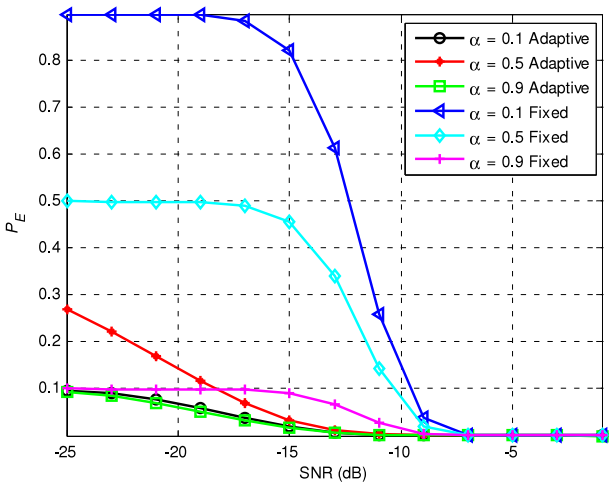

Fig. 3. P_E against variations in SNR γ.

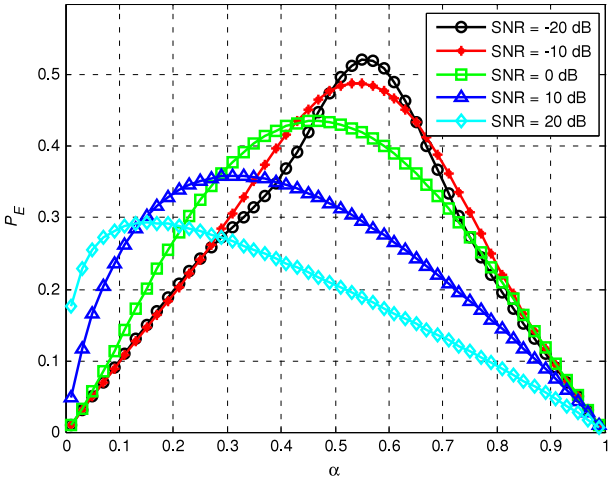

Fig. 2. P_E against variations in utilization factor α.

of [8]). Therefore, the outcomes illustrated in this paper are intuitively assumed to be more persuasive compared to other findings given elsewhere. Whatever the case is, an AT policy consequently needs to be appropriately developed to address SNR variations. Such a task can be administered by having the results of (17) substituted in (15) for predefined probability metrics and the active spectrum reuse can be attained as in (14) accordingly.

The second simulation exercise is on examining the total error decision probability P_E against variations of α values in the range 0 to 1, and for wider range of arbitrary SNR values -20 dB, -10 dB, 0 dB, 10 dB and 20 dB, as depicted in Fig. 2. The noise variance is $\sigma_w^2 = 1$ and the prefixed threshold value fixed to have CFAR or P_{FA} of 0.01. This value is commonly used in line with the maximum acceptable figure of 0.1 for both the P_{FA} and P_{MD} defined in the IEEE 802.22 regulation [3]. A higher P_E means lower spectrum efficiency for both the PUs and SUs and vice versa is true. Therefore, P_E needs to be minimized to the best extent as possible to have enhanced spectrum performance. Fig. 2 shows that the worst case scenario for P_E occurs around $\alpha = 0.5$, especially for lower SNR values. That means there is no preference of distinguishing between SUs or PUs while accessing and using particular bands. On the other hand, the best P_E performance, and thus the spectrum utilization, can be achieved on either side of the depicted convex curves. That is lower α values can be assigned for either function of having better SUs' spectrum utilization or higher α values for PUs to enjoy better protection against opportunistic bands access. The shifting of such convex shapes towards the left side of Fig. 2 for higher SNR is also obvious. This is attributed to the enhanced signal and channel condition that allows for better PUs detection under almost a very wide range of α values much below 0.5. Therefore under such higher SNR range above 0 dB, a better spectrum utilization and PUs protection is always achievable.

The third exercise is devoted to examining the proposed adaptive and the classical fixed P_E performances against SNR variations and with respect to arbitrary utilization factors, as shown in Fig. 3. It shows that worst case performance, or higher P_E, occurs at $\alpha = 0.1$ or far below 0.5 and particularly at smaller SNR ranges. At such ranges, the only way to improve the P_E performance is by making the utilization factor much higher than 0.5 such as $\alpha = 0.9$ or above. The P_E for $\alpha = 0.9$ shows a much improved performance as shown in the same figure. The first scenario means no solid protection for PUs, while the second indicates exactly the opposite. As for $\alpha = 0.5$, the P_E is obviously exhibiting poor performance and the trend of which just lies in the center between other trends for $\alpha = 0.1$ and 0.9.

As that is said on the fixed threshold, the AT on the other hand enhances the overall P_E performance to significant levels. This is true in as much as α takes on values either smaller than or larger than 0.5. Again, the P_E performance for $\alpha = 0.5$ is modest; however, it is still much better than the fixed threshold situation, as shown in Fig. 3. A precaution needs always be considered whether to make further PUs protection or allow SUs to flexibly access and use vacant spectrum without paying

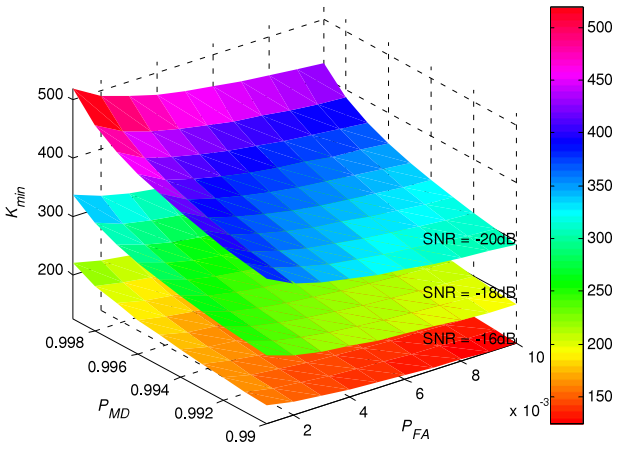

Fig. 4. Minimum sensing duration against variations in (P_{MD}, P_{FA}) and selected SNR γ values.

full attention to PUs' activities in the same or adjacent bands. This can only be decided by allocating a proper utilization factor α, either much greater or less than 0.5 for any of the above situations, respectively.

The fourth and last exercise is around demonstrating the minimum sequence samples required for SS to meet the permissible optimum frame duration. Fig. 4 shows that the minimum samples condition constitutes nonlinear hyperplanes of two arguments, namely the pair (P_{MD}, P_{FA}). Multiple non-overlapping hyperplanes are also obvious for different SNR values. Three arbitrary SNR values of -20 dB, -18 dB and -16 dB, typical in SS environment are assumed. The IEEE 802.22 mandated ranges for CFAR and CDR values are conformed in this example. As predictably exhibited in Fig. 4, the hyperplanes foci are greatly reduced relevant to the increase in SNR values and hence less sample points can realize the minimum of optimum detection frames. On the other hand, larger sample extents are entailed for utterly deteriorated SNR conditions. The minimum sample points are displayed on the K_{min} axis of Fig. 4, which signify the peaks of hyperplanes computed for the targeted lesser values of (P_{MD}, P_{FA}) pair.

As for the design pair (P_{MD}, P_{FA}), smaller setting values entail fairly larger number of sample points to accommodate efficient SS application, especially under inferior SNR circumstances. Recall from the experimental settings of $L = 3$ Slepian tapers and equipped with 2×2 MIMO stated earlier in this section, it becomes well discerned that the value of $K = 1024$ can easily achieve any targeted pair (P_{MD}, P_{FA}) shown in Fig. 4. Hence, it is always advisable to engage an acceptable range of sample points that can attain the minimum OFD demand without further complexity overheads.

7. Conclusion

A systematic paradigm of augmenting the non-parametric MTM with MIMO structures, where the resulting algorithm is named MTSE–MIMO, is thoroughly studied in this paper. The prime intention of such amalgamation ingredients is to enhance the SE performance in CR systems. The related analytical expressions and closed-form performance indicators are developed under flat-fading Rayleigh and AWGN channels. The approach of predefined CFAR and CDR settings is adopted to derive the statistical asymptotes essential for detection AT. The minimum number of sequence points required for the OFD interval is compiled as well. An arbitrary utilization factor ranging from 0 to 1 is engaged into the total decision error probability expression. The simulation exercises corroborated the given analysis and signified on the criticality of implementing particular AT and OFD policies aiming at better PUs and SUs protection and hence spectrum utilization and throughput. This can be attended by assigning an appropriate utilization factor to achieve tradeoff between one of the aforesaid targets.

References

[1] C.R. Stevenson, G. Chouinard, Z. Lei, W. Hu, S.J. Shellhammer, W. Caldwell, IEEE 802.22: The first cognitive radio wireless regional area network standard, IEEE Commun. Mag. (2009) 130–138.

[2] S. Haykin, Cognitive radio: Brain-empowered wireless communications, IEEE J. Sel. Areas Commun. 23 (2) (2005) 201–220.

[3] T. Yucek, H. Arslan, A survey of spectrum sensing algorithms for cognitive radio applications, IEEE Commun. Surv. Tutor. 11 (1) (2009) 116–130. 1st Quarter.

[4] B. Wang, K. Liu, Advances in cognitive radio networks: A survey, IEEE J. Sel. Top. Signal Process. 5 (1) (2011) 5–23.

[5] E.H.G. Yousif, T. Ratnarajah, M. Sellathurai, Modeling and performance analysis of multitaper detection using phase-type distributions over MIMO fading channels, IEEE Trans. Signal Process. 63 (22) (2015) 5882–5896.

[6] Q. Zhang, Multitaper based spectrum sensing for cognitive radio: Design and performance, in: Proc. of VTC, 15–18 May 2011, Yokohama, pp. 1–5.

[7] N. Wang, Y. Gao, X. Zhang, Adaptive spectrum sensing algorithm under different primary user utilizations, IEEE Commun. Lett. 17 (9) (2013) 1838–1841.

[8] S. Zhang, Z. Bao, An adaptive spectrum sensing algorithm under noise uncertainty, in: Proc. IEEE ICC, 5–9 Jun. 2011, Kyoto, pp. 1–5.

[9] Y.-C. Liang, Y. Zeng, E.C.Y. Peh, A.T. Hoang, Sensing-throughput tradeoff for cognitive radio networks, IEEE Trans. Wireless Commun. 7 (4) (2008) 1326–1337.

[10] M. Guerrini, L. Rugini, P. Banelli, Sensing-throughput tradeoff for cognitive radios, in: Proc. of SPAWC, 16–19 Jun. 2013, Darmstadt, pp. 115–119.

[11] V.-D. Nguyen, O.-S. Shin, Cooperative prediction-and-sensing based spectrum sharing in cognitive radio networks, IEEE Trans. Cogn. Commun. Netw. 4 (1) (2018) 108–120.